^{18}F-FDG Imaging: Pitfalls and Artifacts*

Mohei M. Abouzied, MD; Elpida S. Crawford, MS; and Hani Abdel Nabi, MD, PhD

Nuclear Medicine Department, University at Buffalo, Buffalo, New York

^{18}F-FDG PET is emerging as a useful tool in the staging and restaging of many malignant neoplasms, such as lymphoma, lung cancer, colorectal cancer, head and neck cancer, breast cancer, and melanoma. To accurately interpret ^{18}F-FDG findings one must be familiar with the normal physiologic distribution of the tracer, frequently encountered physiologic variants, and benign pathologic causes of ^{18}F-FDG uptake that can be confused with a malignant neoplasm. The objectives of this article are to (a) describe the mechanism of ^{18}F-FDG uptake, (b) list the patient preparation and pertinent patient history before ^{18}F-FDG imaging, (c) describe the whole-body physiologic distribution of ^{18}F-FDG, (d) list and discuss normal physiologic variants, and (e) list and discuss benign pathologic causes of ^{18}F-FDG uptake.

Key Words: ^{18}F-FDG imaging; artifacts

J Nucl Med Technol 2005; 33:145–155

PET with ^{18}F-FDG is one of the fastest growing techniques in nuclear medicine today. ^{18}F-FDG is an analog of glucose and, as such, a versatile radiopharmaceutical with major applications in oncology, neurology, and cardiology. Clinically, ^{18}F-FDG PET is most widely used for cancer detection. ^{18}F-FDG PET has proven its efficacy in general oncologic imaging. The clinical impact of ^{18}F-FDG PET has been reported for many different tumor types, such as lung tumors, colorectal carcinomas, breast carcinoma, and lymphomas. In an extensive review of the ^{18}F-FDG PET literature from 1993 to 2000 comprising 419 articles, the overall sensitivity and specificity was estimated to be 84% and 86%, respectively, and the results from ^{18}F-FDG PET changed the management in approximately one third of the patients (*1*).

PET with ^{18}F-FDG is approved by the Center for Medicare and Medicaid Services for diagnosing, staging, and restaging lung cancer, colorectal cancer, lymphoma, melanoma, head and neck cancer, and esophageal cancer.

Tumor imaging with ^{18}F-FDG is based on the fact that malignant tumors with high metabolic rates take up greater amounts of glucose and ^{18}F-FDG than surrounding tissues.

PET has several advantages over other imaging modalities in cancer detection. Many forms of cancer are systemic and whole- body imaging with ^{18}F-FDG provides a way to monitor extent and progression of the disease. Also, because biochemical changes in a tumor occur before morphologic changes, PET has the potential to provide diagnostic information earlier than CT or MRI.

^{18}F-FDG is administered intravenously and is then transported into cells by glucose transporter proteins in a fashion similar to that for unlabeled D-glucose. Numerous malignant tumors express higher numbers of specific membrane transport proteins, with greater affinity for glucose than normal cells, which permits increased glucose flow into the cancerous cells (*2*).

Subsequently, ^{18}F-FDG is then phosphorylated by hexokinase to form ^{18}F-FDG-6-phosphate. The cell membrane is impermeable to both glucose 6-phosphate and FDG-6-phosphate. However, the latter cannot be further degraded via the glycolysis pathway nor can it easily undergo dephosphorylation by glucose-6-phosphatase. Ultimately, ^{18}F-FDG-6-phosphate remains trapped within the cell and the more ^{18}F-FDG within the cells the more increased uptake within the tumor itself (*3*). To a certain extent, the increased localization usually correlates with more aggressive tumors and greater numbers of viable tumor cells (*4,5*).

Tumor cells are, however, not the only cells that exhibit an increased uptake of ^{18}F-FDG. Recently, Maschauer et al. (*6*) have shown a contribution of the endothelial cells within the tumors and vascular lesions to ^{18}F-FDG uptake, which can be enhanced by endothelial cytokine (vascular endothelial growth factor or VEGF). VEGF stimulates the proliferation and migration of vascularly derived endothelial cells and is overexpressed in a variety of tumors, including renal, breast, ovary, and colon cancer (*6*).

For correspondence or reprints contact: Elpida S. Crawford, MS, Nuclear Medicine Department, University at Buffalo, 105 Parker Hall, 3435 Main St., Buffalo, NY 14214-3007.

E-mail: esc@buffalo.edu

*NOTE: FOR CE CREDIT, YOU CAN ACCESS THIS ACTIVITY THROUGH THE SNM WEB SITE (http://www.snm.org/ce_online) THROUGH SEPTEMBER 2006.

TABLE 1
Patient Preparation

1. Fasting—nothing by mouth for 4–6 h
2. No strenuous exercise 24 h before PET
3. Check blood glucose level (ideally between 120 and 150 mg/dL)
4. Start intravenous line for ^{18}F-FDG administration
5. During circulation time, the patient should rest on a cart or recliner
6. Patient should void before scanning
7. Remove any metallic objects
8. Make the patient comfortable under the scanner—that is, use head and arm support

TABLE 2
Relevant Patient History and Data

- Surgical history: type, site, date of previous surgery or biopsy, site and types of stomas if present
- Clinical history: complaints, type and site of tumor, date of diagnosis
- Current therapy: chemo/radiotherapy, bone marrow–stimulating factors—for example, granulocyte colony-stimulating factor
- Previous therapy received
- History of trauma or recent falls
- Results of previous radiologic investigations; review the patient's film (CT, MRI, and so forth)

Multiple reports have shown that lesions with a high concentration of inflammatory cells, such as neutrophils and activated macrophages, also show increased ^{18}F-FDG uptake, which can be mistaken for malignancy in patients with proven or suspected cancer (*4*). Animal studies have shown that inflammatory cells contribute significantly to ^{18}F-FDG uptake in tumors (*7–13*). Using a tumor mouse model, Kubota et al. reported that 29% of ^{18}F-FDG uptake was related to nontumoral tissue (*11*). This observation could explain why normal and noncancerous conditions, such as infection, inflammation, and healing tissues, can also show increased ^{18}F-FDG uptake.

Not all malignant tissues have avidity for ^{18}F-FDG. Some types of cancer tissues with low malignant potential, such as carcinoid tumor, bronchoalveolar cancer, and mucinous adenocarcinoma, use ^{18}F-FDG at the same rate as normal surrounding tissues, leading to failure in identifying these sites of cancers (*7–16*).

To avoid as many confounding and potentially misleading issues as possible when interpreting the scan, certain prerequisites need to be fulfilled before performing any PET study. They are listed in Table 1. The relevant clinical data from the referring physicians and the patient must be collected and all other diagnostic radiologic investigations done before PET should be reviewed. Relevant history and data that must be collected before ^{18}F-FDG PET are listed in Table 2. The oncologic consult should include the reason(s) for requesting the PET study and, in certain circumstances, a limited physical examination is requested to clarify some findings.

Proper quality control, imaging, and reconstruction are essential for optimal resolution and scan interpretation. The technologist performing the scan should note and record any excessive patient motion. Consider using a head holder to reduce possible motion in head and neck cancer imaging (Fig. 1). Also, consider increasing the acquisition time for both emission and transmission scans in overweight patients to improve the image quality.

HEAD AND NECK

Brain cortex generally has an intense uptake because glucose is the only source of energy in the brain. ^{18}F-FDG accumulation in the brain is fairly constant and consistent as the brain is known to account for as much as 20% of total-body glucose metabolism in the fasting state. Low-to-moderate ^{18}F-FDG uptake occurs in the tonsils and at the base of the tongue because of physiologic activity associated with the lymphatic tissue in Waldeyer's ring.

The presence of ^{18}F-FDG uptake is highly variable (mild or intense) in the salivary glands, including the parotid, submandibular, and sublingual glands (*17*) (Fig. 2). Salivary gland uptake may be symmetric or asymmetric. Asymmetry in the salivary glands could be positional or could be due to

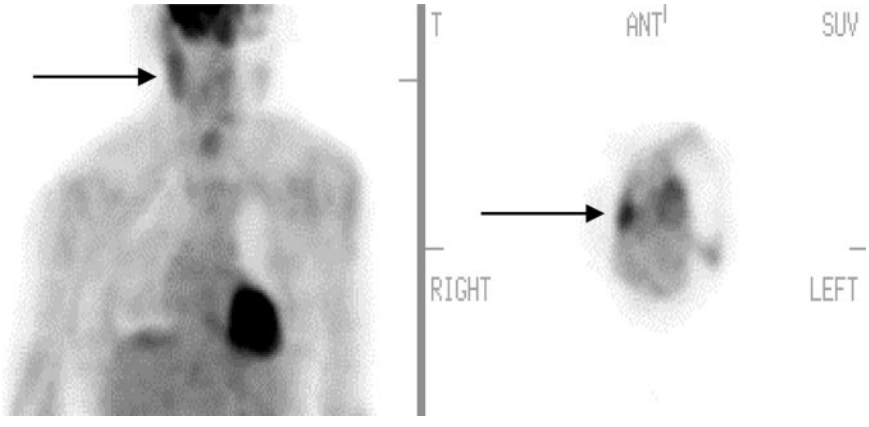

FIGURE 1. Asymmetric salivary gland uptake (projection view). Note increased ^{18}F-FDG uptake in right face/salivary gland and region (arrow) as compared with contralateral side. Patient's head moved during acquisition. SUV = standardized uptake value.

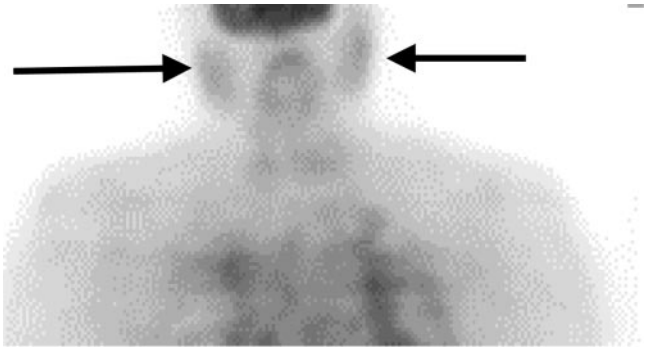

FIGURE 2. Symmetric salivary gland uptake (projection view; arrows) shows mild uptake.

surgical or postradiation therapy inflammatory-induced changes. Radiotherapy can decrease the uptake on the irradiated side.

The extraocular muscles, muscles of the oral cavity, and laryngeal muscles accumulate ^{18}F-FDG with varying degrees. A moderate amount of uptake can be seen in the anterior part of the floor of the mouth due to the genioglossus muscle, which prevents the tongue from falling back in supine patients. If a patient grinds the teeth or chews, the muscles of mastication may appear very prominent. Excessive talking after injection can cause prominent ^{18}F-FDG uptake within the larynx. The laryngeal uptake is normally very subtle, appearing in the form of an inverted V shape. Focal unilateral uptake within the larynx could be due to muscle overuse as in the case of contralateral vocal cord paralysis (*18*) (Fig. 3).

Usually the thyroid uptake is negligible; ranging from no accumulation to mild uptake. Incidental increased ^{18}F-FDG uptake in the thyroid can be seen in about 2% of scans (*19*). Such uptake could be diffuse as in thyroiditis or Graves' disease (Fig. 4). Focal uptake can occur with autonomously functioning thyroid nodules and thyroid malignancies. Patients with focal uptake in the region of the thyroid should be further evaluated because of a higher risk of the finding being associated with malignancy (*20*) (Fig. 5).

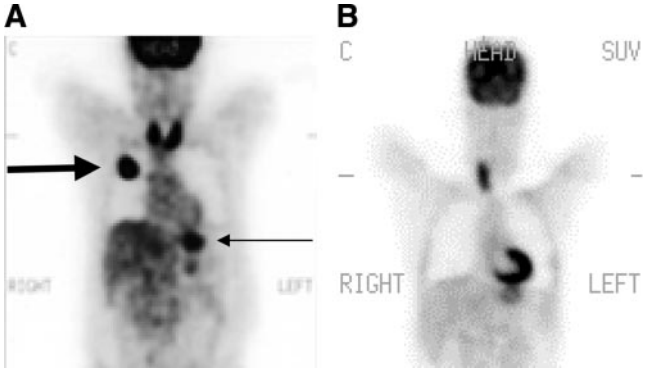

FIGURE 4. Thyroid inflammation. (A) Patient with known squamous cell carcinoma of upper lobe of right lung (thick arrow) who was being evaluated for initial staging. Note intense thyroid uptake due to Hashimoto's thyroiditis. Also note normal stomach uptake (thin arrow). (B) A 57-y-old woman with history of breast carcinoma and left thyroidectomy who was being evaluated because of rising levels of tumor markers. Neck uptake was due to Hashimoto's thyroiditis, which could easily have been mistaken for nodal uptake. C = coronal.

MYOCARDIUM

The myocardial uptake can vary significantly from one patient to another and in the same patient imaged on different occasions. During the fasting state, the myocardium depends on fatty acids to produce energy (*21*). For this reason we should not expect to see much myocardial uptake. On the other hand, in the postprandial state, the myocardial uptake could be enhanced significantly (Figs. 6A–6C). However, in spite of the patient's fasting, we see many variations in the uptake, which range from absent to very intense uptake within the left ventricle, and occasionally we see intense uptake within the right ventricle as well. In some pathologic conditions we see even atrial uptake (Fig. 6B).

Sometimes the heart is not recognized for what it is. Inhomogeneous myocardial uptake and segmental absence

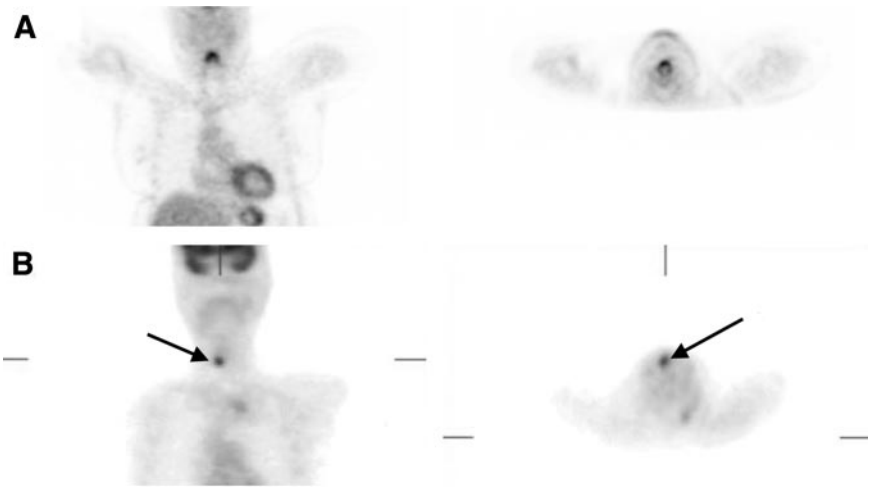

FIGURE 3. Laryngeal uptake. (A) Normal symmetric uptake in larynx. (B) Focal unilateral (arrows). Coronal view on left; transaxial view on right.

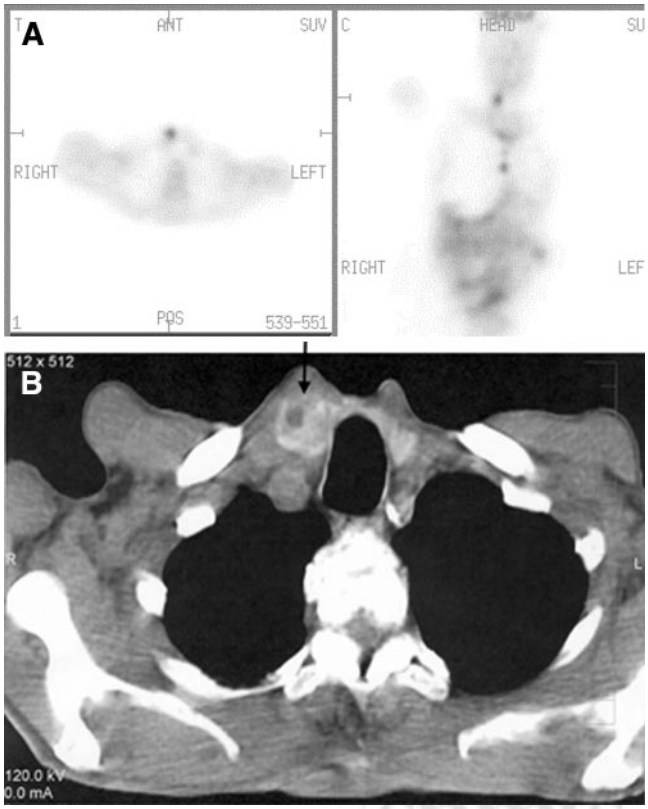

FIGURE 5. Focal thyroid uptake. (A) Focal thyroid uptake seen in right lobe of thyroid gland corresponding to focal density (arrow) seen on CT scan (B). ANT = anterior; POS = posterior; C = coronal.

of uptake attributed to previous myocardial infarction and scar formation (Fig. 6C) can cause confusion when interpreting the study.

GASTROINTESTINAL TRACT

The origin of ^{18}F-FDG uptake in the digestive tract is unknown; possible causes are active smooth muscle, metabolically active mucosa, swallowed secretions, or colonic microbial uptake (*22*). Gastric activity can be seen and has a characteristic J-shape within the left upper abdomen. The uptake can be faint or it can be intense (Fig. 7). Although less common, esophageal activity can

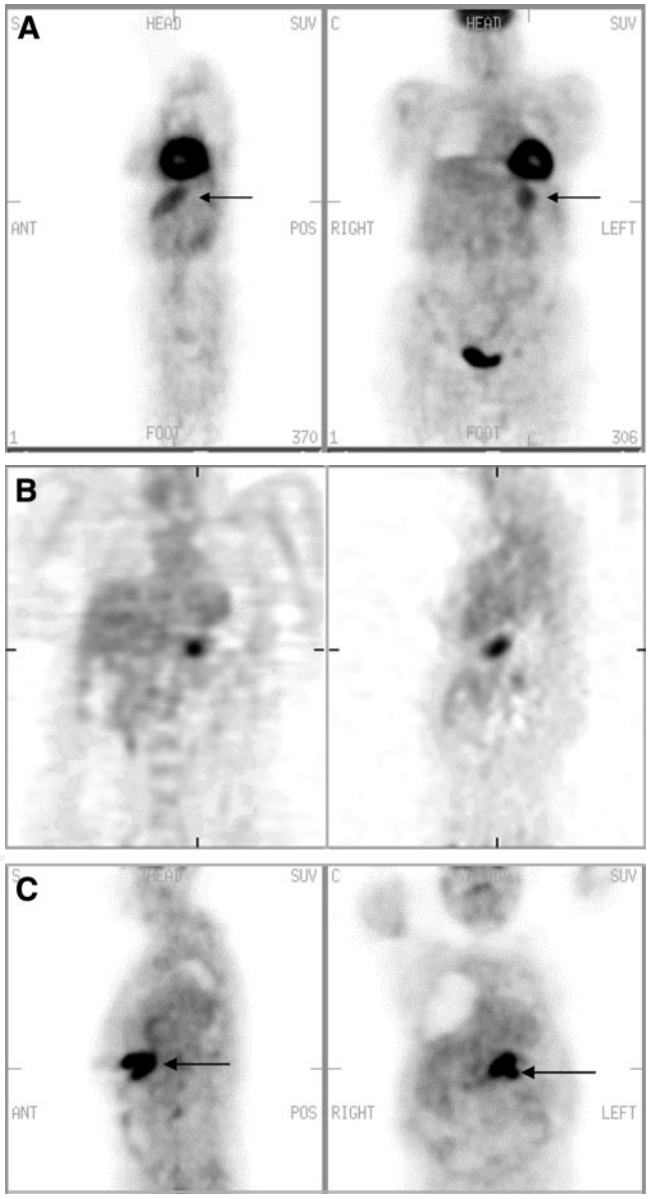

FIGURE 7. Stomach uptake. (A) Normal uptake: mild diffuse uptake (arrows) conforming to stomach configuration. (B) Adenocarcinoma of stomach: focal uptake in region of stomach. Coronal view on left; sagittal view on right. (C) Stomach lymphoma: intense focal uptake (arrows). S = sagittal; C = coronal; ANT = anterior; POS = posterior.

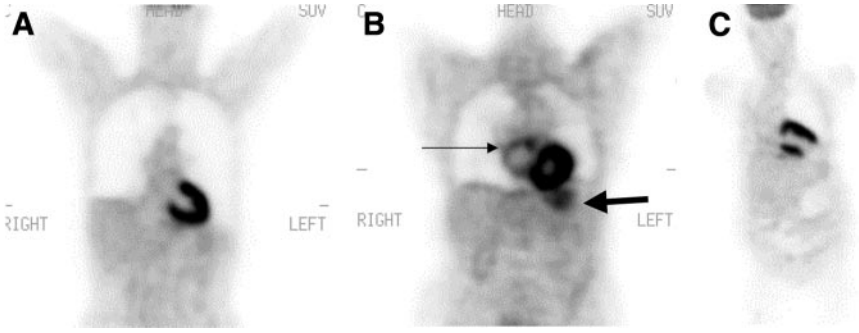

FIGURE 6. (A) Cardiac uptake: Normal physiologic intense ^{18}F-FDG uptake throughout myocardium. (B) Atrial uptake: Note inhomogeneous mild ^{18}F-FDG uptake in enlarged right atrium resembling abnormal mediastinal nodal tissue uptake. Thick arrow points out normal stomach uptake. (C) Cardiac uptake: Apical scar with aneurismal formation.

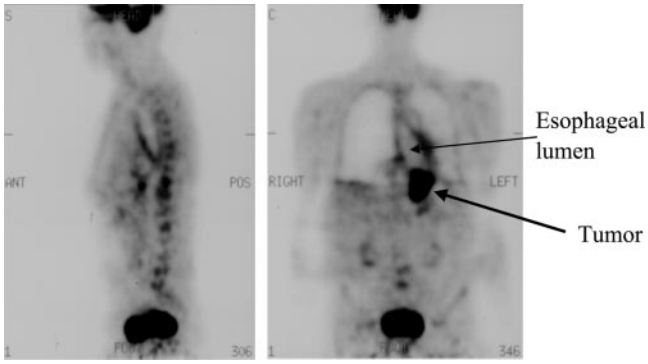

FIGURE 8. Dilated esophagus. A 72-y-old man with known esophageal carcinoma. Note dilated esophagus with linear increased uptake on both sides. Chronic dilation is due to distal obstruction by tumor mass. Linear uptake is due to reactive inflammation. ANT = anterior; POS = posterior; S = sagittal; C = coronal.

be seen as a mild linear uptake anterior to the spine, mostly due to swallowed saliva and partially due to smooth muscle metabolism. Prominent esophageal uptake is abnormal (Figs. 8 and 9). The colonic activity is also variable, ranging from faint heterogeneous activity, to mild focal, segmental, or diffuse activity (Fig. 10). Uptake in the cecum and right colon is usually higher than the rest of the colon because of the abundance of the lymphocyte cells, which are very glucose avid (Fig. 11). However, focal intense activity in the colon should be further evaluated with colonoscopy to exclude a neoplastic process. In some patients, the colonic uptake can cause a great clinical challenge, especially in the lower rectal region. By reviewing the sagittal and the rotating images, one can, in most cases, eliminate any pathologic uptake. The liver uptake is mostly faint and homogeneous. An overlapping loop of bowel can occasionally resemble a focal liver lesion; reviewing the corresponding CT slice can easily differentiate between the 2 conditions.

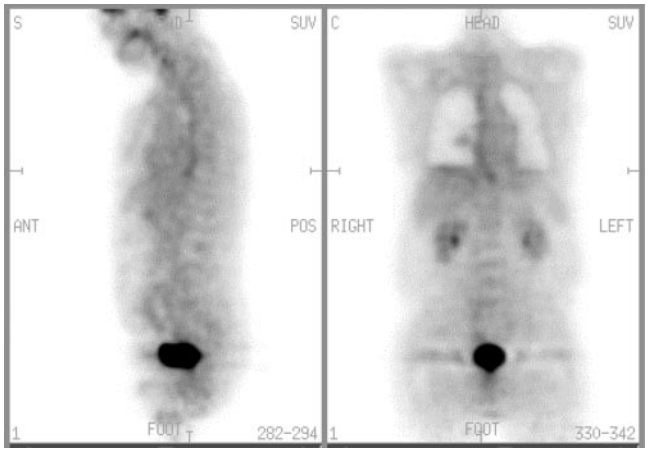

FIGURE 9. Esophageal uptake. Esophageal uptake in patient with gastroesophageal reflux disease. S = sagittal; C = coronal; ANT = anterior; POS = posterior.

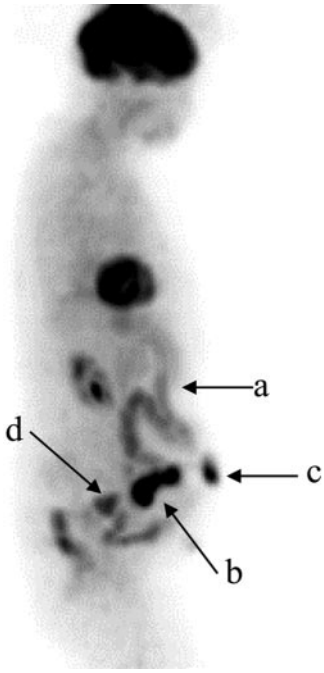

FIGURE 10. Colonic activity (projection view). Patient had bladder cancer, status post cystostomy, and ileal conduit. PET was done to rule out pelvic recurrence. Note nonspecific diffuse colonic activity (a), ileal conduit (b), urinary bag (c), and area of recurrence (d).

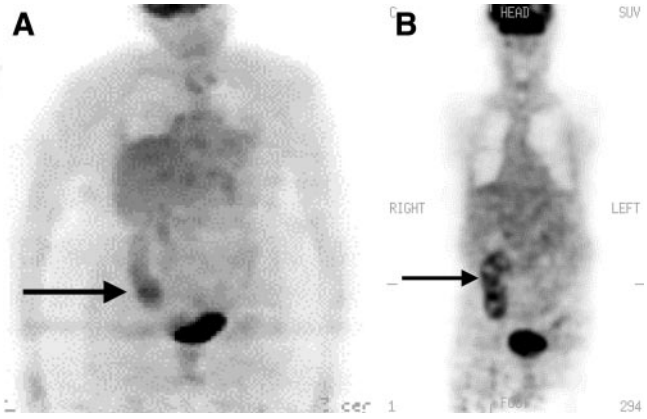

FIGURE 11. Cecal uptake. (A and B) Normal diffuse physiologic uptake (arrow) in cecum. C = coronal.

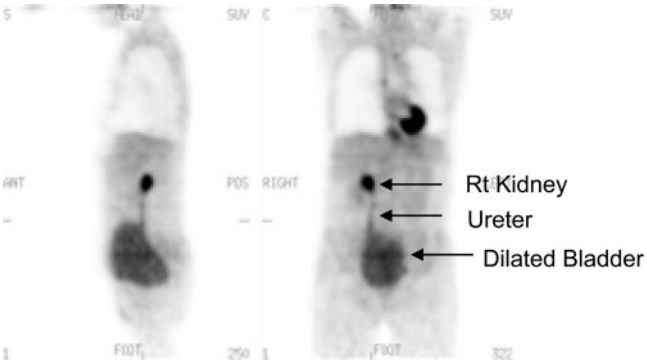

FIGURE 12. Dilated urinary bladder. Note prominent right (Rt) kidney collecting system, right ureter, and dilated urinary bladder.

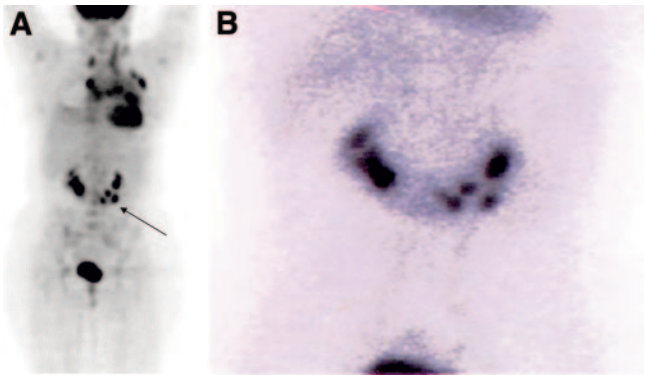

FIGURE 13. Horseshoe kidney. (A) Horseshoe kidney (arrow) seen on ^{18}F-FDG PET scan (projection view on left). Patient with Hodgkin's lymphoma. (B) ^{99m}Tc-Glucoheptonate scan confirms presence of horseshoe kidney.

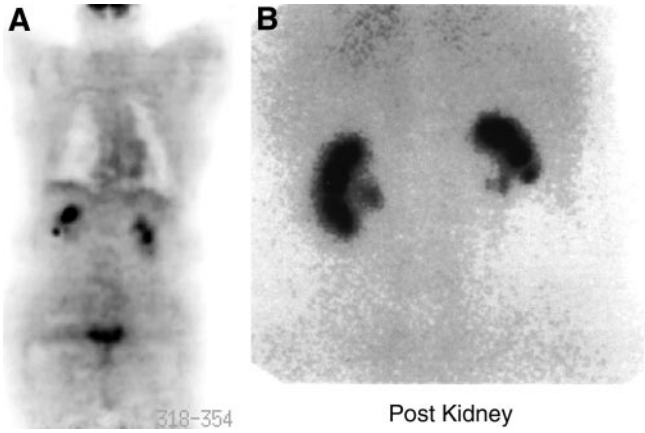

FIGURE 14. Renal activity. (A) Intense activity in right kidney collecting system overlapping right lobe of liver, simulating a liver lesion. (B) ^{99m}Tc-Dimercaptosuccinic acid image of same patient confirms that right kidney is slightly higher than left. Post = posterior.

GENITOURINARY

Because FDG is filtered through the glomeruli, without reabsorption unlike glucose, one should see the activity within the collecting system, ureters, and urinary bladder.

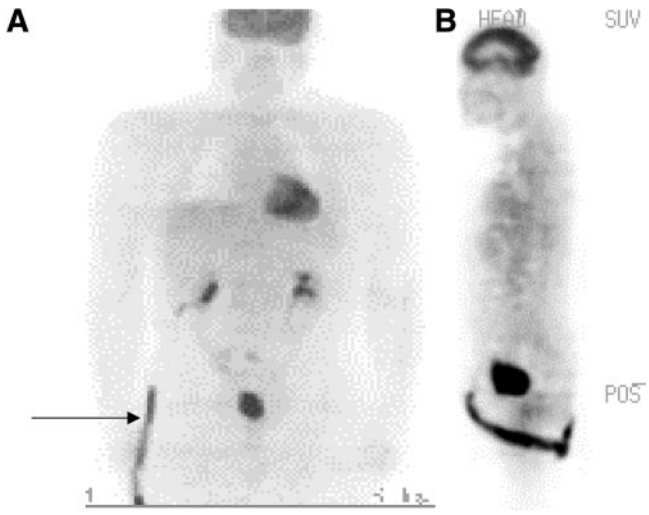

FIGURE 16. (A) Nephrostomy tube (arrow). (B) Diaper artifact. POS = posterior.

Hydration and frequent voiding promote diuresis and help to decrease the radiation dose to the genitourinary tract. Congenital urinary malformation and acquired structural deformity as in postsurgical intervention can create artifacts (Figs. 12, 13, 14, and 15).

For example, a horseshoe kidney, congenital pelvic kidney, and transplanted kidney can simulate neoplastic lesions. Furthermore, focal urinary activity within the ureter can also simulate focal nodal neoplasia. One must also be aware of urine contamination and surgical tubes draining the kidney (Fig. 16).

Increased ^{18}F-FDG uptake has been reported in the normal uterus during menstruation (*23,24*), in a follicular ovarian cyst (*25*), and in the ovary with an inflammatory reaction during ovulation (*26*). In a recent study by Nishizawa et al. (*27*), the authors observed distinct ovarian ^{18}F-FDG uptake with an SUV of 3.9 ± 0.7 in 26 of 32 premenopausal women examined during the late follicular to early luteal phase of the menstrual cycle. Eighteen of the 32 women also showed focal ^{18}F-FDG uptake in the endometrium, with an SUV of 3.3 ± 0.3.

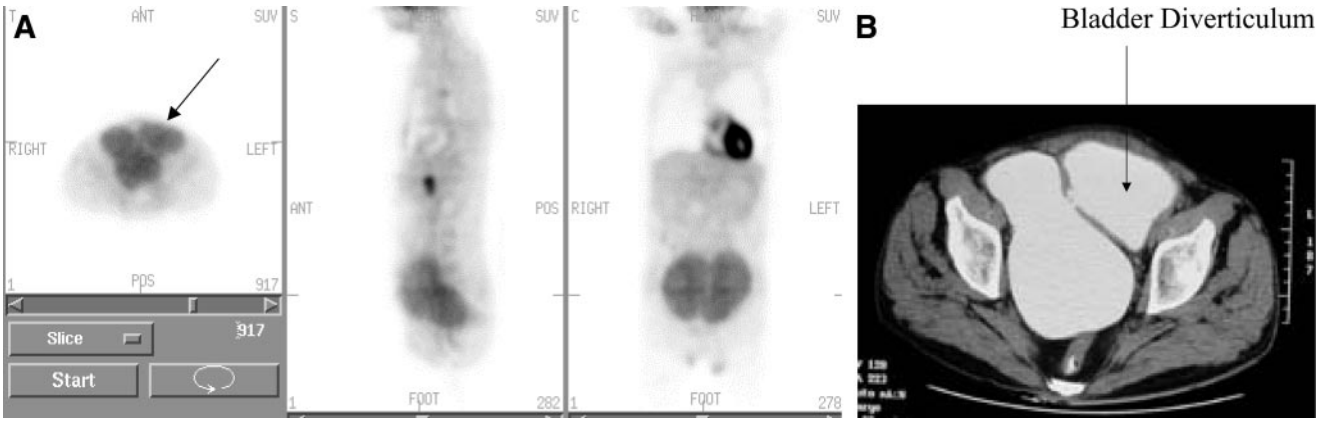

FIGURE 15. Bladder diverticulum. (A) Bladder diverticulum caused by chronic bladder outlet obstruction by hypertrophied prostate. (B) Corresponding CT scan. ANT = anterior; POST = posterior; S = sagittal; C = coronal.

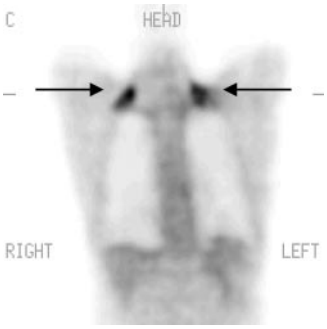

FIGURE 17. Muscle uptake. Symmetric muscle uptake in neck (arrows). C= coronal.

FIGURE 18. Intercostal muscle uptake due to persistent coughing (projection view).

On the other hand, all 9 women in the first 3 d of the menstrual cycle demonstrated intense ^{18}F-FDG uptake in the endometrium, with an SUV of 4.6 ± 1.0. The authors concluded that in women of reproductive age, ^{18}F-FDG imaging should preferably be done within a week before or a few days after the menstrual flow phase to avoid any misinterpretation of pelvic ^{18}F-FDG PET images (*27*).

MUSCULAR ACTIVITY

Vigorous exercise in the days just before a scan can cause intense uptake in the associated skeletal muscles. Skeletal muscle uptake could be enhanced not only because of exercise activity but also because of stress-induced muscle tension as is often seen in the trapezius and paraspinal muscles. Hyperventilation may induce uptake in the diaphragm as well.

Muscle uptake is typically symmetric, mild-to-moderate linear activity (Figs. 17 and 18). However, occasionally the uptake can be focal and unilateral, which could create a diagnostic challenge, especially in head and neck cancer and lymphoma. Similarly, the use of insulin to adjust the serum glucose level immediately before injection of ^{18}F-FDG can result in ^{18}F-FDG accumulation in skeletal muscle. Benzodiazepines may be used to decrease paraspinal and posterior cervical muscle uptake in tense patients.

In addition to the muscles, increased ^{18}F-FDG uptake can be seen in the adipose tissue of the neck, supraclavicular regions, around the large vessels in the mediastinum, the axillae, the perinephric regions, and in the intercostal spaces along the thoracic spine in 3.7% of patients undergoing ^{18}F-FDG PET, constituting a potential source of false-positive PET (*28*). Uptake in the neck adipose tissue is typically bilateral and symmetric, intense, and more often multifocal than linear (*29*) (Fig. 19).

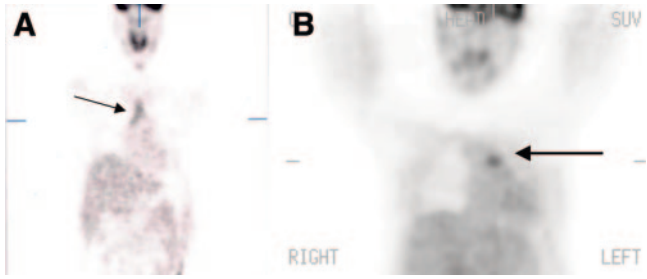

FIGURE 20. Thymus uptake (coronal views). (A) Diffuse thymus uptake (arrow). (B) Focal thymus uptake (arrow).

THYMUS UPTAKE

Thymus uptake is a normal finding in children and young adults, appearing as an upside down letter V. Also, thymus hyperplasia after chemotherapy is a normal variant in the adult population as well (*25,30*) (Fig. 20).

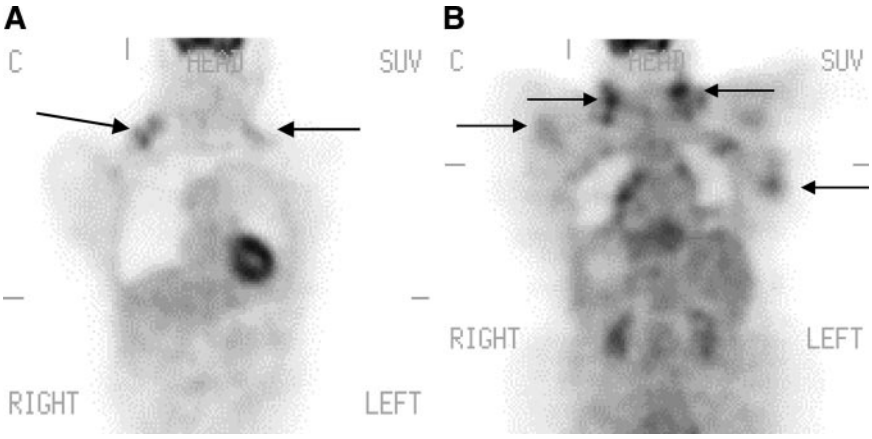

FIGURE 19. Brown fat uptake. (A) Asymmetric neck uptake (arrows). (B) Intense symmetric uptake in adipose tissue (arrows). Brown fat can cause difficulty in scan interpretation. C = coronal.

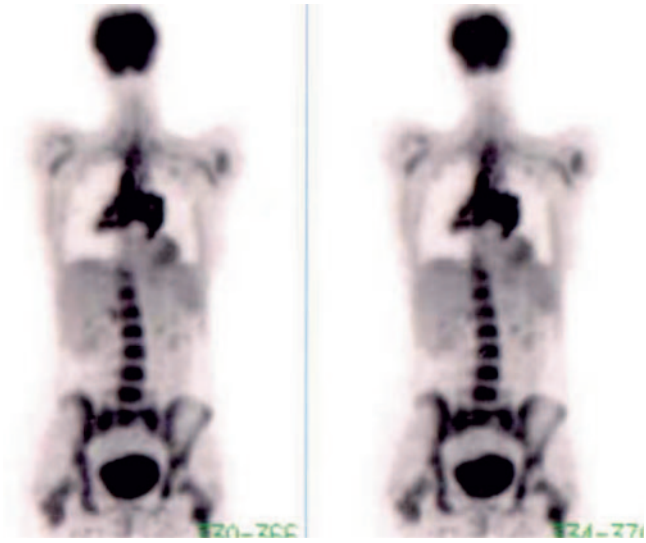

FIGURE 21. Bone marrow. Intense ^{18}F-FDG uptake in bone marrow is attributed to hematopoietic growth factor.

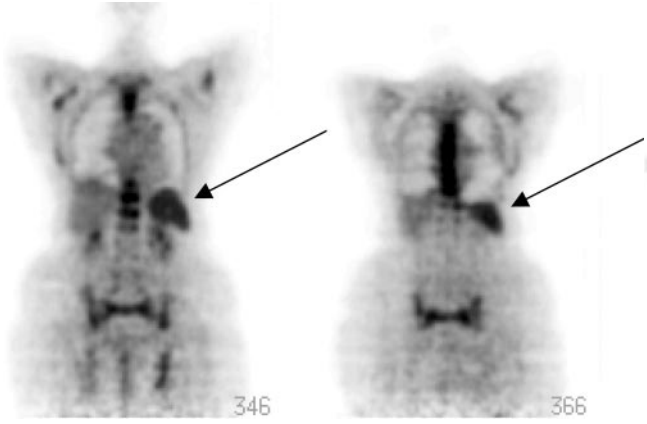

FIGURE 22. Spleen uptake (arrows) due to hematopoietic growth factor.

FIGURE 23. ^{18}F-FDG uptake in lymph nodes attributed to tuberculosis (projection view).

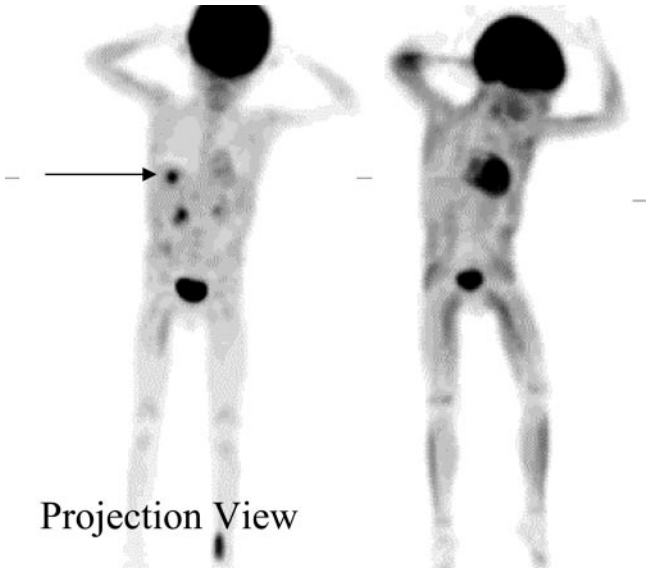

FIGURE 24. Fungal infection in liver of pediatric patient. (A) Before therapy (arrow). (B) Infection resolved on image after specific antifungal therapy.

BONE MARROW

Bone marrow accumulation of ^{18}F-FDG is generally faint diffuse low-grade activity, less than liver activity and mostly seen in vertebral bodies. Focal activity within bone marrow is always suspicious for an abnormality. Uniform diffuse increased bone marrow activity can be seen also with bone marrow recovery after chemotherapy, which usually resolves by 1 mo after therapy (*31*).

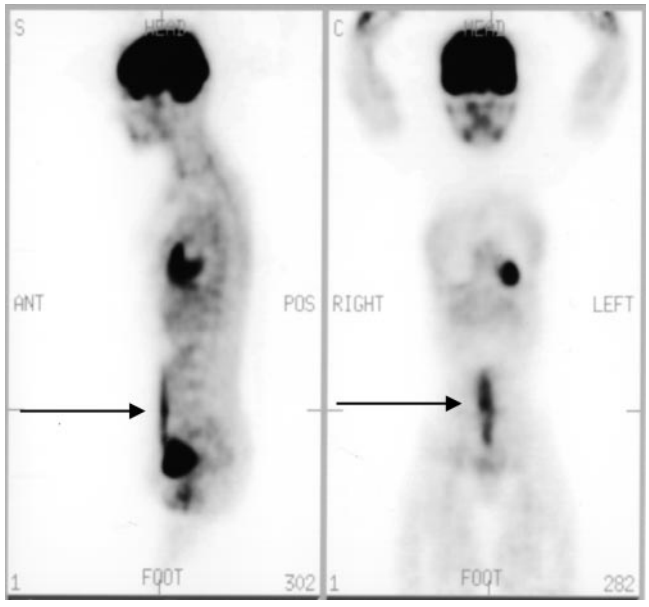

FIGURE 25. Scar tissue from recent surgery. Patient underwent recent abdominal surgery for hernia repair. Note linear superficial increased ^{18}F-FDG uptake along anterior abdominal wall conforming to abdominal scar tissue (arrow). S = sagittal; C = coronal; ANT = anterior; POS = posterior.

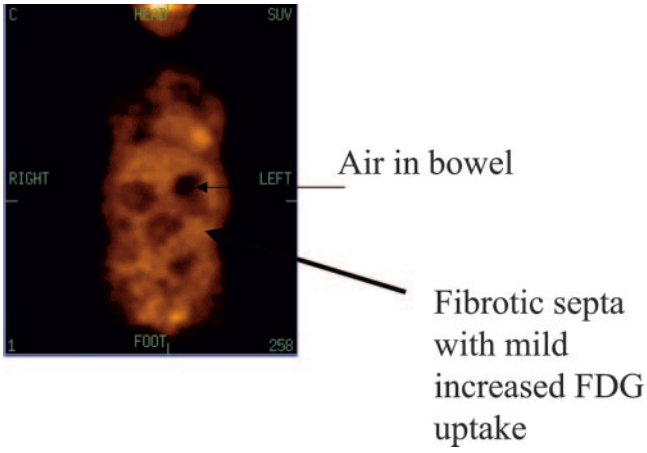

FIGURE 26. Abdominal fibrosis, honeycomb appearance. Patient had history of multiple abdominal surgeries leading to scattered segmental fibrosis. Image shows mild ^{18}F-FDG uptake between dilated loops of bowel forming the honeycomb appearance. C = coronal.

Increased diffuse intense ^{18}F-FDG uptake in the bone marrow (Fig. 21) has been reported in patients taking hematopoietic growth factors (HGF), granulocyte–macrophage colony-stimulating factor (GM-CSF), granulocyte colony-stimulating factor (G-CSF), and erythropoietin (*31,32*). In a study by Yao et al. (*33*), administration of G-CSF caused ^{18}F-FDG uptake to increase to 97% above baseline on day 3 of therapy and to 170% above baseline on day 10 of therapy. Sugawara et al. showed that ^{18}F-FDG uptake of bone marrow declined after G-CSF was completed but remained higher than baseline for almost 4 wk after completion of G-CSF (*31*). The identification of bone metastases could be a challenging task in this group of patients. Therefore, depending on the clinical situation, waiting for 2–4 wk before performing the ^{18}F-FDG study is advised.

SPLENIC UPTAKE

Normally, there is faint uptake of ^{18}F FDG in the spleen. Because the spleen is an active site for the extramedullary hematopoiesis, one would expect to see a diffuse enhanced ^{18}F-FDG uptake in conjunction with diffuse bone marrow uptake after administration of HGF, such as G-CSF and erythropoietin (Fig. 22) (*32,34*). Similarly; other hematologic diseases such as thalassemia, which can cause extramedullary hematopoiesis, can also lead to enhanced ^{18}F-FDG uptake in the spleen (*35*). Furthermore, other nonneoplastic conditions such as infection can cause diffuse enhancement of glucose uptake within the spleen.

BENIGN PATHOLOGIC CAUSES OF ^{18}F-FDG UPTAKE

^{18}F-FDG is not a tumor-specific probe. In addition to its physiologic accumulation in different organs, it can accumulate in nonneoplastic pathologic conditions, including infection (*36–40*), whether acute or chronic infection such as tuberculosis, granulomatous diseases such as sarcoidosis (*38,41,42*), and autoimmune disease such as Grave's disease (*43,44*) (Figs. 23 and 24). In addition, the ^{18}F-FDG uptake can be enhanced by inflammatory induced changes, which include postoperative healing scars and postradiation therapy (Figs. 25, 26, 27, and 28). A unique example of an inflammatory condition is the one caused by the atherosclerotic plaque formation that is associated with an abundance of macrophages known by its avidity to ^{18}F-FDG (*45–47*) (Fig. 29). The degree of

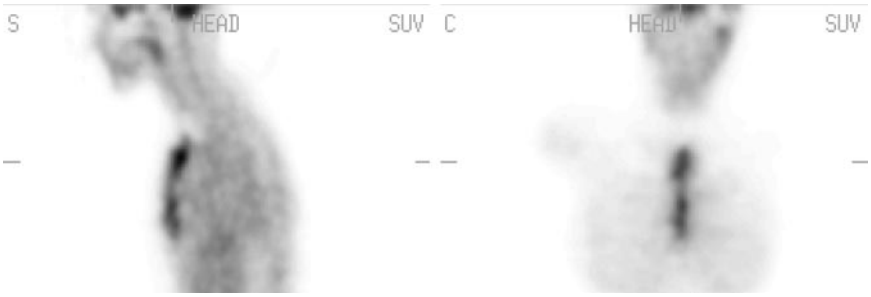

FIGURE 27. Uptake in sternum after coronary artery bypass grafting. Patient had open-heart surgery 1 wk before ^{18}F-FDG study. S = sagittal; C = coronal.

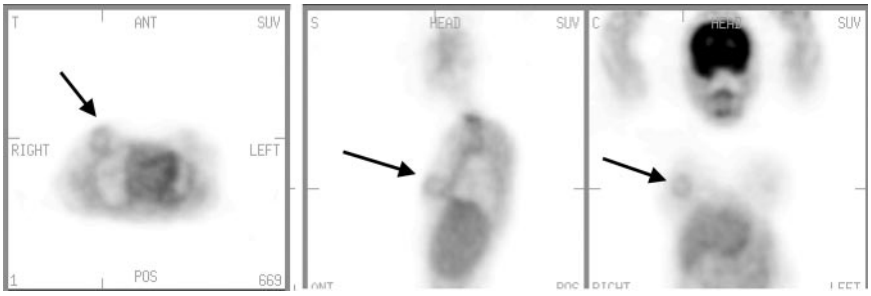

FIGURE 28. Postsurgical hematoma (arrows). Patient had excisional breast biopsy 10 d before ^{18}F-FDG scan. ANT = anterior; POS = posterior; S = sagittal; C = coronal.

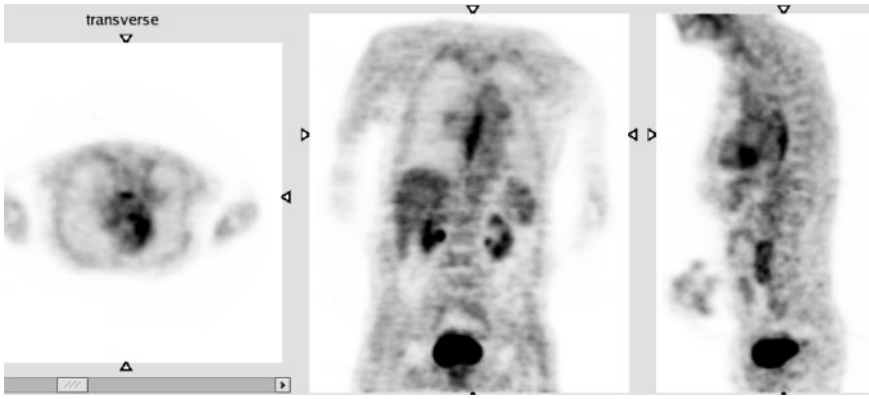

FIGURE 29. Intense aortic uptake due to inflammation (unstable plaque formation).

uptake is usually less than the uptake within the neoplastic tissues. However, there is clearly an overlap between the 2 conditions and, in some cases, the uptake could even exceed the neoplastic uptake. Furthermore; the image interpreter should be aware of a high accumulation of ^{18}F-FDG in some benign tumors, such as giant cell tumor, fibrous dysplasia of the bone, and adenomatous polyps in the colon (*48,49*).

Occasionally one will also see breast-related activity. Breast activity will be more obvious in lactating females (Fig. 30).

CONCLUSION

In recent years ^{18}F-FDG PET has become an essential tool in the management of cancer patients. To optimize its appropriate interpretation, one must understand the normal physiologic distribution and different confounding artifacts. Proper patient preparation and a complete patient history are needed to accurately interpret the scan and also to avoid the artifacts.

ACKNOWLEDGMENTS

The authors acknowledge the following technologists: Paul Galantowicz, Scott Wisniewski, Debbie Erb, and Kimberly Dix. Also, images in Figures 3B, 18, and 23 are courtesy of Drs. Jayakumari Gona and Dr. Syed Husain at the Western New York Veterans Healthcare Hospital System.

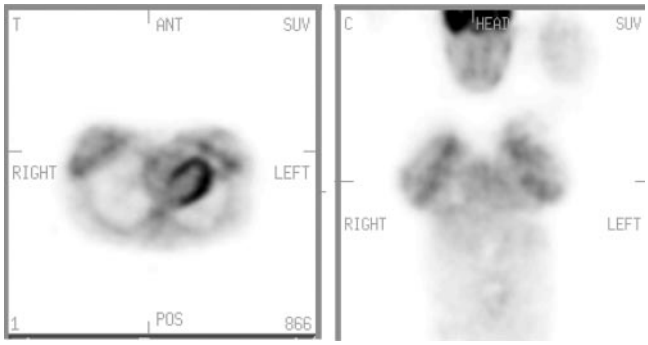

FIGURE 30. Breast uptake, lactating female. ANT = anterior; POS = posterior; C = coronal.

REFERENCES

1. Gambhir SS, Czernin J, Schwimmer J, et al. A tabulated summary of the FDG PET literature. *J Nucl Med.* 2001;42(suppl):1S–93S.
2. Wahl RL. Targeting glucose transporters for tumor imaging: "sweet" idea, "sour" result. *J Nucl Med.* 1996;37:1038–1041.
3. Pauwels EK, Ribeiro MJ, Stoot JH, et al. FDG accumulation and tumor biology. *Nucl Med Biol.* 1998;25:317–322.
4. Brown RS, Leung JY, Fisher S, et al., Intratumoral distribution of tritiated-FDG in breast carcinoma: correlation between glut-1 expression and FDG uptake. *J Nucl Med.* 1996;37:1042–1047.
5. Higashi K, Clavo AC, Wahl RL. Does FDG uptake measure proliferative activity of human cancer cells? In vitro comparison with DNA flow cytometry and tritiated thymidine uptake. *J Nucl Med.* 1993;34:414–419.
6. Maschauer S, Prante O, Hoffmann M, Deichen JT, Kuwert T. Characterization of ^{18}F-FDG uptake in human endothelial cells in vitro. *J Nucl Med.* 2004;45:455–460.
7. Kim BT, Kim Y, Lee KS, et al. Localized form of broncheoalveolar carcinoma: FDG PET findings. *AJR.* 1998;170:935–939.
8. Fenchel S, Grab D, Nuessle K, et al. Asymptomatic adnexal masses: correlation of FDG PET and histopathologic findings. *Radiology.* 2002;223:780–788.
9. Higashi K, Ueda Y, Sakurai A, et al. Correlation of Glut-1 glucose transporter expression with [^{18}F]FDG uptake in non-small cell lung cancer. *Eur J Nucl Med.* 2000;27:1778–1785.
10. Zhung H, Alavi A. 18-Fluorodeoxyglucose positron emission tomographic imaging in the detection and monitoring of infection and inflammation. *Semin Nucl Med*. 2002;32:47–59.
11. Kubota K, Matsuzawa T, Fujiwara T, et al. Differential diagnosis of lung tumor with positron emission tomography: a prospective study. *J Nucl Med.* 1990;31:1927–1932.
12. Brown RS, Leung JY, Fisher SJ, Frey KA, Ethier SP, Wahl RL. Intratumoral distribution of tritiated fluorodeoxyglucose in breast carcinoma. I. Are inflammatory cells important? *J Nucl Med.* 1995;36:1854–1861.
13. Kubota R, Yamada S, Kubota K, Ishiwata K, Tamahashi N, Ido T. Intratumoral distribution of fluorine-18-fluorodeoxyglucose in vivo: high accumulation in macrophages and granulation tissues studied by microautoradiography. *J Nucl Med.* 1992;33:1972–1980.
14. Whiteford MH, Whiteford HM, Yee LF, et al. Usefulness of FDG-PET scan in the assessment of suspected metastatic or recurrent adenocarcinoma of the colon and rectum. *Dis Colon Rectum*. 2000;43:759–767.
15. Higashi K, Ueda Y, Seki H, et al. Fluorine-18-FDG PET imaging is negative in bronchioloalveolar lung carcinoma. *J Nucl Med.* 1998;39:1016–1020.
16. Gould MK, Maclean CC, Kuschner WG, Rydzak CE, Owens DK. Accuracy of positron emission tomography for diagnosis of pulmonary nodules and mass lesions: a meta-analysis. *JAMA*. 2001;285:914–924.
17. Goerres GW, von Schulthess GK, Hany TF. Positron emission tomography and PET CT of the head and neck: FDG uptake in normal anatomy, in benign lesions, and in changes resulting from treatment. *AJR*. 2002;179:1337–1343.
18. Kamel EM, Goerres GW, Burger C, von Schulthess GK, Steinert HC. Recurrent laryngeal nerve palsy in patients with lung cancer: detection with PET-CT image fusion: report of six cases. *Radiology*. 2002;224:153–156.
19. Kang KW, Kim S-K, Kang H-S, et al. Prevalence and risk of cancer of focal thyroid incidentaloma identified by ^{18}F-fluorodeoxyglucose positron emission tomography for metastasis evaluation and cancer screening in healthy subjects. *J Clin Endocrinol Metab*. 2003;88:4100–4104.

20. Bruel AVA, Maes A, Potter T, et al. Clinical relevance of thyroid fluorodeoxyglucose-whole body positron emission tomography incidentaloma. *J Clin Endocrinol Metab*. 2002;87:1517–1520.
21. Neely JR, Morgan HE. Relationship between carbohydrate and lipid metabolism and the energy balance of heat muscle. *Annu Rev Physiol.* 1974; 36:413–459.
22. Shreve PD, Anzai Y, Wahl RL. Pitfalls in oncologic diagnosis with FDG PET imaging: physiologic and benign variants. *RadioGraphics.* 1999;19: 61–77.
23. Yasuda S, Ide M, Takagi S, Shohtsu A. Intrauterine accumulation of F-18 FDG during menstruation. *Clin Nucl Med.* 1997;22:793–794.
24. Chander S, Meltzer CC, McCook BM. Physiologic uterine uptake of FDG during menstruation demonstrated with serial combined positron emission tomography and computed tomography. *Clin Nucl Med.* 2002;27:22–24.
25. Cook GJ, Fogelman I, Maisey MN. Normal physiological and benign pathological variants of 18-fluoro-2-deoxyglucose positron-emission tomography scanning: potential for error in interpretation. *Semin Nucl Med.* 1996;26:308–314.
26. Gordon BA, Flanagan FL, Dehdashti F. Whole-body positron emission tomography: normal variations, pitfalls, and technical considerations. *AJR.* 1997;169:1675–1680.
27. Nishizawa S, Inubushi M, Okada H. Physiological ^{18}F-FDG uptake in the ovaries and uterus of healthy female volunteers. *Eur J Nucl Med Mol Imaging*. December 2004 [Epub ahead of print].
28. Cohade C, Karen A, Mourtzikos KA, Wahl R. "USA-Fat": prevalence is related to ambient outdoor temperature—evaluation with ^{18}F-FDG PET/CT. *J Nucl Med*. 2003;44:1267–1270.
29. Cohade C, Osman M, Pannu HK, Wahl RL. Uptake in supraclavicular area fat ("USA-Fat"): description on ^{18}F-FDG PET/CT. *J Nucl Med*. 2003;44:170–176.
30. Ferdinand B, Gupta P, Kramer EK. Spectrum of thymic uptake at ^{18}F-FDG PET. *Radiographics*. 2004;24:1611–1616.
31. Sugawara Y, Fisher SJ, Zasadny KR, Kison PV, Baker LH, Wahl RL. Preclinical and clinical studies of bone marrow uptake of fluorine-18-fluorodeoxyglucose with or without granulocyte colony-stimulating factor during chemotherapy. *J Clin Oncol.* 1998;16:173–180.
32. Blodgett TM, Ames JT, Torok FS, McCook BM, Meltzer CC. Diffuse bone marrow uptake on whole-body F-18 fluorodeoxyglucose positron emission tomography in a patient taking recombinant erythropoietin. *Clin Nucl Med*. 2004;29:161–163.
33. Yao WJ, Hoh CK, Hawkins RA, et al. Quantitative PET imaging of bone marrow glucose metabolic response to hematopoietic cytokines. *J Nucl Med.* 1995;36:794–799.
34. Abdel-Dayem HM, Rosen G, El-Zeftawy H, et al. Fluorine-18 fluorodeoxyglucose splenic uptake from extramedullary hematopoiesis after granulocyte colony-stimulating factor stimulation. *Clin Nucl Med.* 1999;24:319–322.
35. Wong CL, Fulham MJ. Increased splenic FDG uptake on PET in beta-thalassemia. *Clin Nucl Med*. 2004;29:266–267.
36. Sumpe KD, Dazzi H, Schaffner A, von Schulthess GK. Infection imaging using whole-body FDG-PET. *Eur J Nucl Med*. 2000;27:822–832.
37. Alavi A, Gupta N, Alberini JL, et al. Positron emission tomography imaging in nonmalignant thoracic disorders. *Semin Nucl Med*. 2002;32: 293–321.
38. Bakheet SM, Powe J, Ezzat A, et al. F-18-FDG uptake in tuberculosis. *Clin Nucl Med.* 1998;23:739–742.
39. Bicik I, Bauerfeind P, Breitbach T, et al. Inflammatory bowel disease activity measured by positron-emission tomography. *Lancet.* 1997;350:262.
40. Lewis PJ, Salama A. Uptake of fluorine-18-deoxyglucose uptake in sarcoidosis. *J Nucl Med.* 1994;35:1647–1649.
41. Yasuda S, Shothsu A, Ide M, et al. High fluorine-18-deoxyglucose uptake in sarcoidosis. *Clin Nucl Med*. 1996;21:983–984.
42. Chen YK, Chen YL. Elevated F-18 FDG uptake in the thymus in Graves' disease. *Clin Nucl Med*. 2003;28:142–143.
43. Boerner AR, Voth E, Theissen P, Wienhard K, Wagner R, Schicha H. Glucose metabolism of the thyroid in Graves' disease measured by F-18-fluoro-deoxyglucose positron emission tomography. *Thyroid*. 1998;8:765–772.
44. Yun M, Yeh D, Araujo LI, Jang S, Newberg A, Alavi A. F-18 FDG uptake in the large arteries: a new observation. *Clin Nucl Med.* 2001;26:314–319.
45. Yun M, Jang S, Cucchiara A, Newberg AB, Alavi A. ^{18}F-FDG uptake in the large arteries: a correlation study with the atherogenic risk factors. *Semin Nucl Med.* 2002;32:70–76.
46. Rudd JH, Warburton EA, Fryer TD, et al. Imaging atherosclerotic plaque inflammation with [^{18}F]-fluorodeoxyglucose positron emission tomography. *Circulation.* 2002;105:2708–2711.
47. Aoki J, Watanabe H, Shinozaki T, et al. FDG PET of primary benign and malignant bone tumors: standardized uptake value in 52 lesions. *Radiology*. 2001;219:774–777.
48. Kamel E, Thumshirn M, Truninger K, et al. Significance of incidental ^{18}F-FDG accumulations in the gastrointestinal tract in PET/CT: correlation with endoscopic and histopathologic results. *J Nucl Med*. 2004;45:1804–1810.